BJR https://doi.org/10.1259/bjr.20210473

Received: 14 April 2021 | Revised: 25 May 2021 | Accepted: 27 May 2021

Cite this article as:
Decabooter E, Swinnen ACC, Öllers MC, Göpfert F, Verhaegen F. Operation and calibration of the novel PTW 1600SRS detector for the verification of single isocenter stereotactic radiosurgery treatments of multiple small brain metastases. *Br J Radiol* 2021; **94**: 20210473.

FULL PAPER

Operation and calibration of the novel PTW 1600SRS detector for the verification of single isocenter stereotactic radiosurgery treatments of multiple small brain metastases

[1]ESTHER DECABOOTER, MSc, [1]ANS CC SWINNEN, [1]MICHEL C ÖLLERS, [2]FABIAN GÖPFERT and [1]FRANK VERHAEGEN

[1]Department of Radiation Oncology (Maastro clinic), GROW School for Oncology, Maastricht University Medical Centre+, Maastricht, The Netherlands
[2]PTW Freiburg, Freiburg, Germany

Address correspondence to: Mrs Esther Decabooter
E-mail: *esther.decabooter@maastro.nl*

Objectives: The aim of this work was to evaluate the operation of the 1600SRS detector and to develop a calibration procedure for verifying the dose delivered by a single isocenter stereotactic radiosurgery (SRS) treatment of small multiple brain metastases (BM).
Methods: 14 clinical treatment cases were selected with the number of BM ranging from 2 to 11. The dosimetric agreement was investigated between the calculated and the measured dose by an OCTAVIUS 1600SRS array detector in an OCTAVIUS 4D phantom equipped with dedicated SRS top. The cross-calibration procedure deviated from the manufacturer's as it applied field sizes and dose rates corresponding to the volumetric modulated arc therapy segments in each plan.
Results: Measurements with a plan specific cross-calibration showed mean ± standard deviation (SD) agreement scores for cut-off values 50%, 80%, 95%, of 98.6 ± 1.7%, 96.5 ± 4.6%, 97.3 ± 4.4% for the 6 MV plans respectively, and 98.6 ± 1.5%, 96.6 ± 4.0% 96.4 ± 6.3%, for the 6 MV flattening filter free (FFF) plans respectively. Using the default calibration procedure instead of the plan specific calibration could lead to a combined systematic dose offset of 4.1% for our treatment plans.
Conclusion: The 1600SRS detector array with the 4D phantom offers an accurate solution to perform routine quality assurance measurements of single isocenter SRS treatments of multiple BM. This work points out the necessity of an adapted cross-calibration procedure.
Advances in knowledge: A dedicated calibration procedure enables accurate dosimetry with the 1600SRS detector for small field single isocenter SRS treatment of multiple brain metastases for a large amount of BM.

INTRODUCTION

Patients with multiple brain metastases (BM) are treated with stereotactic radiosurgery (SRS) that used high dose per fraction, and therefore require dedicated equipment, special planning techniques and small treatment margins to achieve high dose conformality.[1,2] A complex linear accelerator (linac) based delivery technique to achieve high dose conformality is volumetric modulated arc therapy (VMAT) where the dose rate, the gantry rotation speed and multileaf collimator (MLC) aperture shape varies dynamically during the arc delivery.[3] A single isocenter technique can be applied to efficiently deliver the dose while requiring less than one-half of the beam time required for multiple isocenter set-ups.[4] The use of single-isocenter non-coplanar beams can further increase the conformity of the treatment plans making them competitive to Gammaknife treatment plans.[5] By using a single isocenter technique, there is an increased risk of geometrical miss. Lesions located further away from the isocenter are more sensitive to rotational set-up errors.[6] For this reason, frameless thermoplastic immobilization masks in combination with daily imaging-based set-up corrections, using cone beam CT (CBCT) in combination with a 6 degrees-of-freedom robotic couch and the use of optical surface tracking systems, are crucial for this irradiation technique.[7–9] Planning target volume (PTV) margins down to 1 mm are appropriate assuming an adequate imaging and/or tracking system.[2,9]

This state-of-the-art irradiation technique for the delivery of highly conformal radiation fields to multiple BM requires efficient and accurate quality assurance (QA) measures and equipment.[10] The dosimetric verification of this irradiation

technique poses several unique challenges such as the highly modulated VMAT plans containing small fields, a volumetric spread of the treatment lesions over the brain volume and treatment plans containing non-coplanar beams. The OCTAVIUS 1000SRS liquid filled 2D ionization chamber (IC) array has been described as an excellent detector for small field dosimetry especially for verifying stereotactic treatments.[11,12] The array detector can be inserted in the OCTAVIUS 4D phantom with the SRS top to perform a three-dimensional (3D) verification. However, the measuring area of the 1000SRS is restricted to 11 × 11 cm^2, and therefore too limited for dose verification of multiple BM in the head. The advanced OCTAVIUS 1600SRS array detector has similar properties but an enlarged active detector of 15 × 15 cm^2 to include all BM in an extended measurement volume. This work aims to study the operation of this novel detector for a relevant number of clinical cases.

As the VMAT plans required for this irradiation technique are typically highly modulated and consist of small subfields shaped by the MLC. The recommended cross-calibration procedure may not be suitable for these treatment plans. The second aim of this work was to develop a dedicated cross-calibration procedure, using the field sizes and dose rates determined for the treatment cases.

METHODS AND MATERIALS

Treatment cases and delivery

Table 1 summarizes 14 clinical SRS treatment cases with number of BM ranging from 2 to 11. The fractionation schemes were determined in accordance with the Dutch guidelines depending on the volume of the largest PTV.[13] Both coplanar and non-coplanar RapidArc treatments using 6 MV flattened as well as unflattened beams were considered during planning, and treatment plan calculation was done with AcurosXB algorithm v. 15.5 (Varian Medical Systems, Palo Alto, CA). A detailed description of the treatment cases and delivery techniques can be found in Supplementary Material 1. The PTVs and the distance to the isocenter are mentioned to illustrate the spatial arrangement of the BM.

Operation procedure of the detector array

The 1600SRS detector is inserted in the OCTAVIUS 4D phantom. Controlled by an inclinometer, the OCTAVIUS 4D phantom rotates synchronously with the gantry, keeping the 1600SRS detector array perpendicular to the beam while taking time- and gantry angle-resolved dose measurements.[14] The measurements were performed using an OCTAVIUS SRS phantom top with a diameter of 17 cm corresponding to a source-to-surface distance (SSD) of 91.5 cm (Figure 1). The OCTAVIUS 1600SRS consists of 1521 liquid-filled IC distributed over an active measurement area of 15 × 15 cm^2. Each detector covers a cross-section of 2.5 × 2.5 mm^2 with a height of 0.5 mm, resulting in an active volume of approximately 0.003 cm^3. The adjacent chambers are distributed heterogeneously with a center-to-center distance of 2.5 mm in the inner area (6.5 × 6.5 cm^2) and 5.0 mm in the outer area (15 × 15 cm^2) (Figure 1). For each treatment plan, the measured dose was reconstructed to a 3D dose volume using the OCTAVIUS 4D dose reconstruction algorithm in VeriSoft, v. 8.0 (PTW-Freiburg, Germany).[14] In the TPS, the treatment plans were projected on the artificial homogeneous phantom CT data set provided with the OCTAVIUS 4D system and recalculated. The electron density of the OCTAVIUS 4D phantom relative to water was set to 1.016 g/cm^3 according to the manufacturer's recommendations.

The OCTAVIUS 4D algorithm uses percentage depth dose (PDD) curves independently measured with an ionization chamber in water at a SSD of 85 cm corresponding to the SSD when using a standard top with a diameter of 32 cm. With a source to isocenter distance of 100 cm, the average SSD for the rotational unit equipped with the SRS top is 92 cm, taking the curved surface into account. Verisoft was used to create new PDD data for a SSD of 92 cm based on the PDD data for a SSD at 85 cm for different field sizes ranging from 1 × 1 cm to 26 × 26 cm^2 defined at the isocenter. Consequently, these PDD data are used to reconstruct dose values along the ray lines that connect the relevant detectors and the focus of the beam.[14] The phantom was positioned at the isocenter using the room lasers and each plan was measured separately at couch rotation zero. For treatment plans with a mixture of coplanar and non-coplanar beams, a dedicated algorithm in Verisoft was used to reconstruct the dose distribution using the actually planned couch angles. To evaluate the dosimetric agreement between the measured and calculated dose a 3D γ evaluation method implemented in Verisoft was used with a (local) γ criterion of 2%/2 mm and cut-off values of 50%, 80% and 95%.[15] This means that voxels with doses below 50%, 80% or 95% of the maximum calculated dose were ignored in the analysis. These values were chosen to encompass most of the irradiated volume, re-evaluate the PTV coverage and focus on the higher dose regions, respectively.

Calibration procedure

To ensure a TPS-independent dose verification, the array detector was cross-calibrated with a pinpoint IC (PTW, Freiburg, Germany) (0.015 cm^3 volume). The dose corresponding to 100 MU (6 MV) and 500 MU (6 MV FFF) in the isocenter was measured using a PMMA insert allowing the pinpoint IC to be positioned at the isocenter within the OCTAVIUS 4D phantom. The dose measurement with the pinpoint IC was corrected with the daily output variation of the linac. A non-negligible dependence of field size and dose-rate on the response of the liquid filled ionization chamber of the 1600SRS detector are described by in literature.[16] Since the treatment plans consist of small field sizes and varying dose rate, especially in the case of the 6 MV FFF treatment plans, the development of an accurate calibration procedure is necessary.The dose-per-pulse dependency of the detector and the volume effects described by Poppe et. al. vary with field size and are especially pronounced for small field sizes.[16]Therefore, PTW recommends to perform the cross-calibration with a field size matching the field size of the clinical plan. For small field sizes, this is typically 5 × 5 cm^2.As the clinical treatment plans in this study contain a lot of very small VMAT segments contributing to the dose distribution, the equivalent field sizes (EFSs) were calculated for all the 14 treatment plans using equation (1) for a rectangular field.[17]

$$EFS = \frac{2 \times L \times W}{W+L} \quad (1)$$

Table 1. Overview of the clinical treatment plans in this study

Plan no.	Amount of PTVs	Fractionation scheme	Treatment technique (couch angles in degrees)	PTVs (cm^3)	Distances of PTV to isocenter (cm)
1	2	3 × 8 Gy	Coplanar (0)	0.59/4.07	6.99/0.78
2	3	3 × 8 Gy	Coplanar (0)	19.35/9.29/2.72	9.32/6.84/0.08
3	4	3 × 8 Gy	Coplanar (0)	17.6/2/0.2	3.44/2.3/4.52/3.81
4	4	3 × 8 Gy	Coplanar(0)+Non-coplanar(270)	2.47/1.44/3.75/1.77	2.75/3.55/4.84/3.78
5	4	1 × 8 Gy	Coplanar(0)+Non-coplanar(270/315/45/90)	2.47/1.44/3.75/1.77	2.75/3.55/4.84/3.78
6	4	1 × 24 Gy	Coplanar (0)	1.04/0.22/0.44/0.11	3.21/5.64/6.96/6.16
7	5	1 × 24 Gy	Coplanar (0)	1.62/0.14/0.2/0.1/0.13	5.39/4.2/5.81/4.98/4.93
8	6	3 × 8 Gy	Coplanar(0)+Non-coplanar(270)	0.25/0.1/2.44/0.21/0.15/0.08	6.87/4.76/3.32/5.47/5.21/4.4
9	7	3 × 8 Gy	Coplanar (0)	23.23/2.15/0.66/0.23/0.13 0.15/0.1	0.12/5.96/2.56/5.89/5.35/5 .764.69
10	8	3 × 8 Gy	Coplanar(0)+Non-coplanar(270)	9.18/3.13/1.58/1.16/0.34/0.170.32/0.12	4.98/5.65/5.57/4.22/5.76/3.81 /5.43/6.58
11	8	3 × 8 Gy	Coplanar(0)+Non-coplanar(270)	17.17/0.53/0.34/0.73/0.57/0.52/0.3/0.1	5.78/4.25/5.23/5.36/6.78/4.8 /6.67/2.37
12	9	3 × 8 Gy	Coplanar (0)	4.17/3.19/3.8/0.97/0.45/0.48/0.16/0.14/0.17	2.74/5.18/2.52/1.57/3.4/4.54/ 4.54/4.89/5.72
13	10	3 × 8 Gy	Coplanar (0)	0.82/0.08/5.47/0.07/0.71/0.71/0.09/0.07/0.82	6.71/4.24/4.49/4.07/3.12/5.7/ 6.9/6.82/5.14/7.34
14	11	1 × 24 Gy	Coplanar(0)+Non-coplanar(270)	0.17/0.25/0.33/0.65/0.24/0.1/0.85/0.35/0.2/0.13/0.14	7.18/6.26/4.82/7.88/1.8/4.99/ 7.58/5.42/7.3/2.9/7.68

PTV, planning target volume.

Figure 1. Top Left: Detector area of the 1600SRS array consisting of an outer 15 × 15 cm^2 area with 5 mm center-to-center distance and an inner 6.5 × 6.5 cm^2 area with a center-to-center distance of 2.5 mm. Top right: A transversal view of the SRS top phantom with a diameter of 17 cm and the cylindrical measurement area corresponding to the area of the detector (15 × 15 cm^2) in red and the inner 6.5 × 6.5 cm^2 area in blue. Bottom left: Views from the flat side-of the Octavius 4D phantom with the projection of the SRS top size (17 × 17 cm^2) and measurement area. Bottom Right: View of the measurement setup with the detector array positioned in the OCTAVIUS 4D phantom equipped with the SRS phantom top. SRS, stereotactic radiosurgery

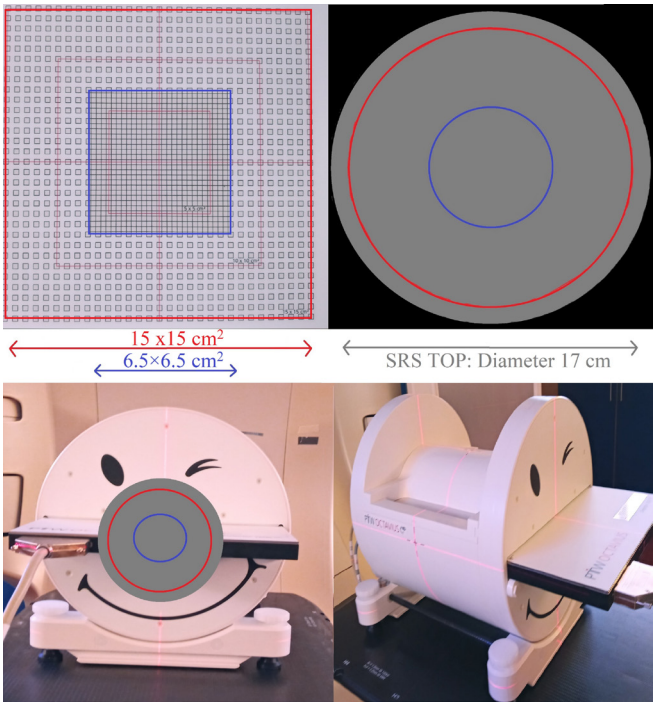

Similar to Wolfs et. al[18], the length (L) in equation (1) was determined by the sum of the projected MLC leaf widths at the isocenter and the width (W) as the average aperture of the MLC leaves forming the field projected at the isocenter. Figure 2 illustrates the distribution of the EFS per treatment plan, for the gantry angles and treatment fields under study. The median EFS (red lines) for all treatment plans was smaller than 2 cm and no VMAT segments (outliers shown as red crosses) exceeded an EFS more than 3.5 cm. Due to the jaw tracking technique the collimator jaws are positioned as close as possible to the outer MLC leaf per control point. As all BM are treated simultaneously with a single isocenter technique, the field sizes shaped by the jaws are always larger than 3 × 3 cm^2.[19] Since the dose is mainly determined by these small field segments created by the MLC, a field size of 2 × 2 cm^2 was chosen to perform the cross-calibration.

Another factor that can have an influence on the response of the detector is the pulse-frequency dependency, which alters with varying dose rate that can cause potential recombination losses in liquid filled IC.[16,20] The dose rate corresponding to the average dose rate over all gantry angles and treatment fields of the plans

Figure 2. Boxplot per clinical treatment plan illustrating the distribution of the EFS for the VMAT segments of the fourteen treatment plans. Median EFS over all VMAT segments are shown as a red line and outliers as red crosses. EFS, equivalent field size; VMAT, volumetric modulated arc therapy

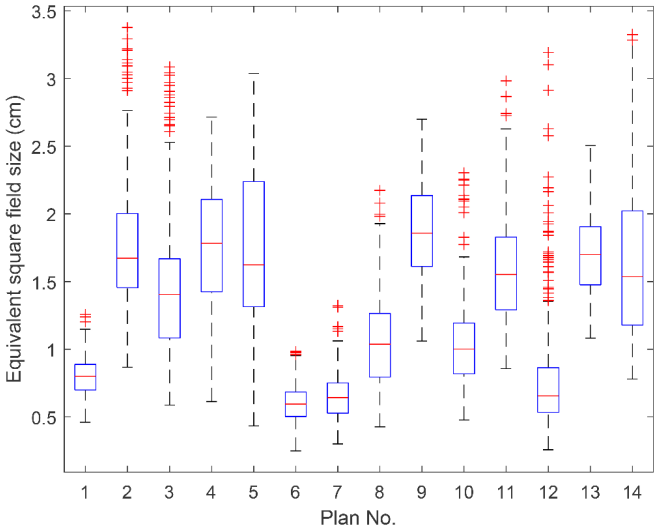

were calculated and summarized in Figure 3. Regarding the 6 MV treatment plans, the dose rate typically stayed constant at the maximum nominal dose rate of 600 MU/min. Larger variations of average dose rates are seen between 6 MV FFF treatment plans. Larger error bars demonstrate larger variations in dose rates within the 6 MV FFF treatment plans, which are due to the limited speed of the gantry rotation. Although the maximum nominal dose rate is 1400 MU/min for 6 MV FFF beams the dose rate is often reduced while the gantry rotation velocity is maximized.

To take these dose rate variations on the detector response into account, the cross-calibration was performed at the nominal dose rate closest to the average dose rate of the treatment plan. Above findings lead to a new calibration procedure consisting of an individualized calibration per treatment plan by delivering 100 MU for 6 MV beams and 500 MU for 6 MV FFF beams using a 2 × 2 cm^2 squared field at gantry zero at the nominal dose rate closest to the average dose rate of the treatment plan (SSD 91.5 cm, depth 8.5 cm).

RESULTS

Table 2 summarizes the influence of the dose rate and field size of the calibration factor used for the treatment plan. A difference in calibration factor up to −2.6% and −2.5% was seen for a 2 × 2 cm^2 field relative to the by the manufacturer recommended 5 × 5 cm^2 field for 6 MV and 6 MV FFF beams respectively. For the lowest used nominal dose rate closest of 800 MU/min, this had an influence of −1.8% on the calibration factor relative to the maximum nominal dose rate of 1400 MU/min. Combining these effects, using a 2 × 2 cm^2 and a dose rate of 800 MU/min relative to the manufacturer's recommendations, can cause a difference up to −4.1% for 6 MV FFF. The influence of the dose-rate dependence is not relevant for 6 MV beams since the dose rate typically stayed constant at the maximum nominal dose rate

Figure 3. Average and standard deviation of dose rate (MU/min) per treatment plan for plans calculated with 6 MV and 6 MV FFF. The error bars indicate the SD of the dose rate (MU/min) for all VMAT segments in the treatment plan. The horizontal lines show the nominal dose rates on our Varian TrueBeam STx for both 6 MV and 6 MV FFF.

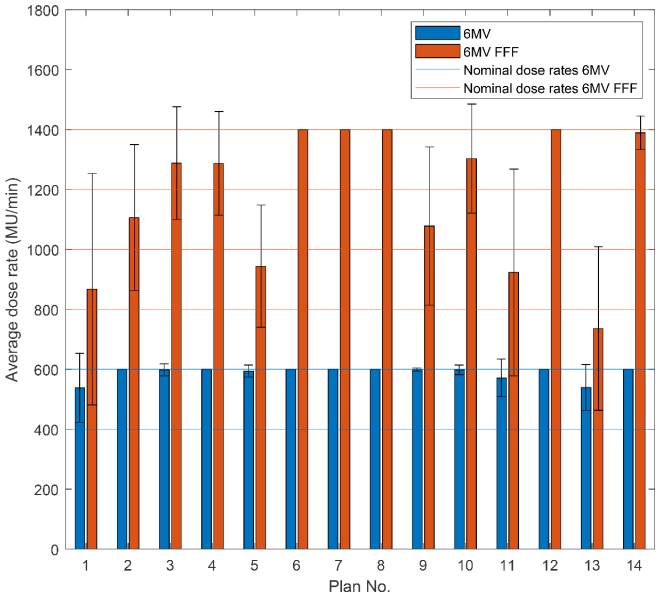

Figure 4. The dosimetric agreement between the measured and calculated dose evaluated using a 3D γ criterion of 2%/2 mm and a cut-off value of 80% for 6 MV (+) and 6 MV FFF (*) with the default calibration in red and the plan specific calibration in blue. The horizontal line indicate the mean agreement score for the default and plan specific calibration respectively. FFF, flattening filter free.

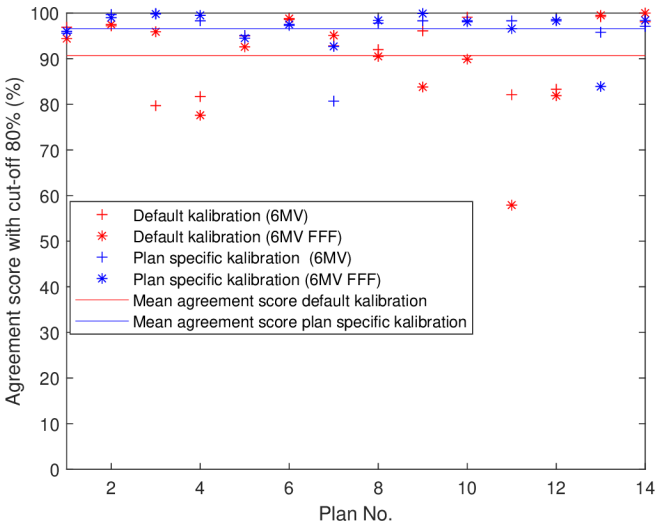

of 600 MU/min in all 14 treatment plans (Figure 3). The relative difference in calibration factors in function of dose rate and field size are summarized in Table 2. The influence of the plan specific calibration on the dosimetric comparison obtained with the OCTAVIUS 1600SRS in the OCTAVIUS 4D phantom with SRS top for the fourteen treatment cases is illustrated in Figure 4. The dosimetric agreement between the measured and calculated dose is evaluated using a 3D γ criterion of 2%/2 mm and a cut-off value of 80%.[21] The agreement scores in red show the scores obtained using a default calibration and the scores in blue the scores obtained using a plan specific calibration. In the latter case, the mean agreement ± standard deviation (SD) improves from 92.3 ± 7% to 96.5 ± 4.6% and from 89.7 ± 11% to 96.6 ± 4% for 6 MV and 6 MV FFF beams respectively.

The comparison between absolute dose calculations and measurements obtained with the OCTAVIUS 1600SRS in the OCTAVIUS 4D phantom with SRS top for 14 treatment cases with 6 MV and 6 MV FFF beams is shown in Tables 3 and 4, respectively. We have found mean ± SD agreement scores of 98.6 ± 1.7%, 96.5 ± 4.6% and 97.3 ± 4.4% (6 MV) and 98.6 ± 1.5%, 96.6 ± 4.0% and 96.4 ± 6.3% (6 MV FFF) for the different cut-off values 50%, 80 and 95% respectively using 3D γ criteria of 2%/2 mm.The relative deviations were defined as the difference between the maximum reference dose calculated by the TPS (TPS D_{max}) and the measured maximum dose (Measured D_{max}), referring to the maximum dose in the 3D measurement volume, divided by the maximum TPS dose. In general, the measurements yield lower results than the doses calculated by the Acuros XB dose calculation algorithm

DISCUSSION

For an accurate treatment of multiple BM with a single isocenter SRS VMAT technique, dedicated QA procedures and equipment are required.[10] Besides an advanced planning technique,[22,23] that requires at least a type B or C calculation algorithm and knowledge of small field dosimetry uncertainties,[24,25] routine machine

Table 2. Difference in calibration factor (%) in function of dose rate and field size for 6 MV and 6 MV FFF relative to a 5 × 5 cm^2 field at the maximum dose rate respectively 600 Mu/min and 1400 Mu/min

	6 MV	6 MV FFF			
Dose rate (MU/min): Field size (cm × cm):	**600**	**800**	**1000**	**1200**	**1400**
2 × 2	−2.6	−4.1	−3.6	−3.1	−2.5
3 × 3	−0.6	−2.7	−2.1	−1.5	−0.9
4 × 4	−0.3	−2.2	−1.6	−1.0	−0.3
5 × 5	x	−1.8	−1.2	−0.6	x

FFF, flatenning filter free.

Table 3. OCTAVIUS 4D measurement results (6 MV) with 3D γ criteria of 2%/2 mm (Agreement score), using cut-off values of 50%, 80%, and 95%

Plan no.	Agreement score (%) cut-off			TPS D_{max} (Gy)	Measured D_{max} (Gy)	$\frac{(TPS\ D_{max} - Measured\ D_{max})}{TPS\ D_{max}}$ (%)
	50%	80%	95%			
1	97.6	95.6	95.8	11.1	10.57	4.8
2	98.8	99.7	98.2	11.2	10.96	2.5
3	99.9	99.9	99.7	10.3	10.19	1.0
4	99.6	98.3	100	9.7	9.46	2.8
5	98.7	95.1	96.6	9.7	9.38	3.0
6	98.6	97.3	83.3	34.5	30.47	11.6
7	92.8	80.7	100	29.7	27.04	9.0
8	99.6	97.8	100	9.7	9.04	6.7
9	99.4	98.3	100	11.0	11.01	0.3
10	99.6	98.3	100	10.9	10.60	2.2
11	99.0	98.3	99.0	10.6	10.08	4.6
12	99.5	98.6	96.2	10.7	10.63	0.3
13	97.8	95.8	93.7	10.6	9.99	5.6
14	98.1	97.1	100	31.9	31.00	2.7

TPS, treatment planning system.
D_{max} (Gy) is the maximum dose calculated by the TPS and measured.

Table 4. OCTAVIUS 4D measurement results (6 MV FFF) with 3D γ criteria of 2%/2 mm, using cut-off values of 50%, 80% and 95% and D_{max} (Gy) the maximum dose in the measurement volume of the OCTAVIUS 4D phantom calculated by the TPS and measured by the array detector

Plan no.	Agreement score (%) cut-off			TPS D_{max} (Gy)	Measured D_{max} (Gy)	$\frac{(TPS\ D_{max} - Measured\ D_{max})}{TPS\ D_{max}}$ (%)
	50%	80%	95%			
1	98.2	96.0	100	10.7	10.42	2.4
2	99.6	99.0	100	10.5	10.50	0.50
3	99.9	99.8	100	10.4	10.08	3.0
4	99.9	99.5	96.3	9.8	9.39	3.9
5	98.5	94.5	95.8	9.9	9.52	3.9
6	97.0	97.5	85.7	35.0	31.05	11.4
7	95.2	92.7	100	33.2	30.20	9.0
8	99.6	98.4	100	9.7	9.11	6.0
9	99.4	99.9	100	11.0	10.97	0.3
10	99.8	98.1	100	10.9	10.77	0.8
11	98.7	96.6	100	10.7	10.33	3.4
12	98.7	98.3	93.5	10.4	10.38	0.6
13	95.8	83.9	78.6	10.8	10.37	3.7
14	99.5	98.4	100	32.3	31.1	3.6

FFF, flatenning filter free; TPS, treatment planning system.

QA assures the correct execution of the mechanical requirements of the treatment technique. Accurate 3D dosimetric verification is the last hurdle for an accurate and safe implementation of the treatment technique.

Since the BM can have very small volumes, down to 0.08 cm^3 according to the treatment plans in this work, a detector with a high spatial resolution is required. Radiochromic films offer high spatial resolution and excellent response characteristics but the experimental evaluation is limited to 2D planes which in most cases covers only part of the BM present in a treatment plan.[26] Another disadvantage of the film procedure is that it is very labor intensive and the results are available the next day at the earliest. The OCTAVIUS 1600SRS array detector, which is the successor of the 1000SRS array detector, has an inner spatial resolution of 2.5 mm with an extended measurement range of 15 × 15 cm^2. Using the 1000SRS detector, only 65% of all BM in our clinical treatment plans under study fit inside the measurement field-of-view (FOV). Due to the expanded measurement range, all except one lesion fit inside the measurement FOV of the 1600SRS detector while maintaining the excellent resolution. The 1600SRS array combined with the OCTAVIUS 4D phantom makes it possible to measure multiple widely spaced target volumes treated with coplanar and non-coplanar beams in a single measurement with immediate results. An accurate cross-calibration is required using set-up conditions that are representative of the VMAT segments in the clinical treatment plans. The field-size dependence of the detector response is taken into account by determining the EFS of the VMAT segments in the treatment plans. For all treatment plans described in this manuscript the median EFS were smaller than 2 cm. A calibration field size of 2 × 2 cm^2 was considered to be small enough to represent the EFS of the VMAT segments in the treatment plans and large enough to avoid errors in calibration due to set-up uncertainty. Similarly, the average dose-rate is used to account for losses due to recombination by performing a cross-calibration at the nominal dose rate closest to the average dose rate of the treatment plan. When these influences are not taken into account this can lead to combined dose differences up to 4.1% for 6 MV FFF beams for our treatment plans. These differences can lead to a systematic shift of the measured dose. Cross-calibrating with a pinpoint IC has the advantage is that the system requires no data input from the linac nor the TPS for the measurement and leads to a completely independent dose verification.[14] A plan specific calibration with the pinpoint IC can also be applied to measurements using the 1000SRS detector because it features similar technology than the 1600SRS detector. For the 14 treatment cases described in this manuscript, the comparison between absolute dose calculations and the measurements yield high agreement scores for both 6 MV and 6 MV FFF energies. This indicates that the described measurement method can be used for a variety of treatment cases ranging in treatment technique, fractionation scheme, amount of BM and spatial arrangement of the BM.

CONCLUSION

The rotational OCTAVIUS 4D phantom in combination with a recently developed high resolution 1600SRS array detector offers an accurate solution to perform routine QA measurements for treatments with multiple BM, which is gaining more attention over the last years. Unlike the recommendation by the manufacturer, we advise that the cross-calibration is performed :

- with a field size corresponding to the average equivalent square field size of the treatment plans;
- with a dose rate corresponding to the average dose rate of the treatment plan per treatment plan.

Otherwise, a systematic dose deviation (in our case up to 4.1%) could occur in the dosimetric verification of single isocenter SRS treatment plans of brain metastases.

ACKNOWLEDGMENTS

The authors would like to thank PTW-Freiburg for providing the OCTAVIUS 1600SRS detector array and for the valuable discussions on the array specifications. Further, we thank Cecile Wolfs and Renate van Doormaal for her help in the specification of equivalent field sizes per clinical treatment plan.

REFERENCES

1. Kraft J, Zindler J, Minniti G, Guckenberger M, Andratschke N. Stereotactic radiosurgery for multiple brain metastases. *Curr Treat Options Neurol* 2019; **21**: 6. doi: https://doi.org/10.1007/s11940-019-0548-3
2. Kirkpatrick JP, Wang Z, Sampson JH, McSherry F, Herndon JE, Allen KJ, et al. Defining the optimal planning target volume in image-guided stereotactic radiosurgery of brain metastases: results of a randomized trial. *Int J Radiat Oncol Biol Phys* 2015; **91**: 100–8. doi: https://doi.org/10.1016/j.ijrobp.2014.09.004
3. Hanna SA, Mancini A, Dal Col AH, Asso RN, Neves-Junior WFP. Frameless image-guided radiosurgery for multiple brain metastasis using VMAT: a review and an institutional experience. *Front Oncol* 2019; **9**(August): 1–11. doi: https://doi.org/10.3389/fonc.2019.00703
4. Clark GM, Popple RA, Young PE, Fiveash JB. Feasibility of single-isocenter volumetric modulated Arc radiosurgery for treatment of multiple brain metastases. *Int J Radiat Oncol Biol Phys* 2010; **76**: 296–302. doi: https://doi.org/10.1016/j.ijrobp.2009.05.029
5. Vergalasova I, Liu H, Alonso-Basanta M, Dong L, Li J, Nie K, et al. Multi-Institutional dosimetric evaluation of modern day stereotactic radiosurgery (SRS) treatment options for multiple brain metastases. *Front Oncol* 2019; **9**(JUN): 1–12. doi: https://doi.org/10.3389/fonc.2019.00483
6. Roper J, Chanyavanich V, Betzel G, Switchenko J, Dhabaan A. Single-Isocenter Multiple-Target stereotactic radiosurgery: risk of compromised coverage. *Int J Radiat Oncol Biol Phys* 2015; **93**: 540–6. doi: https://doi.org/10.1016/j.ijrobp.2015.07.2262
7. Tryggestad E, Christian M, Ford E, Kut C, Le Y, Sanguineti G, et al. Inter- and intrafraction patient positioning uncertainties for intracranial radiotherapy: a study of four frameless, thermoplastic mask-based immobilization strategies using daily cone-beam CT. *Int J Radiat Oncol Biol Phys* 2011;

80: 281–90. doi: https://doi.org/10.1016/j.ijrobp.2010.06.022
8. Tarnavski N, Engelholm SA, Af Rosenschold PM. Fast intra-fractional image-guidance with 6D positioning correction reduces delivery uncertainty for stereotactic radiosurgery and radiotherapy. *J Radiosurg SBRT* 2016; **4**: 15–20.
9. Swinnen ACC, Öllers MC, Loon Ong C, Verhaegen F, Ong CLVF. The potential of an optical surface tracking system in non-coplanar single isocenter treatments of multiple brain metastases. *J Appl Clin Med Phys* 2020; **21**: 63–72. doi: https://doi.org/10.1002/acm2.12866
10. Hartgerink D, Swinnen A, Roberge D, Nichol A, Zygmanski P, Yin F-F, et al. Linac based stereotactic radiosurgery for multiple brain metastases: guidance for clinical implementation. *Acta Oncol* 2019; **58**: 1275–82. doi: https://doi.org/10.1080/0284186X.2019.1633016
11. Bruschi A, Esposito M, Pini S, Ghirelli A, Zatelli G, Russo S. How the detector resolution affects the clinical significance of SBRT pre-treatment quality assurance results. *Phys Med* 2018; **49**: 129–34. doi: https://doi.org/10.1016/j.ejmp.2017.11.012
12. Jeevanandam P, Agnew CE, Irvine DM, McGarry CK. Improvement of off-axis SABR plan verification results by using adapted dose reconstruction algorithms for the Octavius 4D system. *Med Phys* 2018; **45**: 1738–47. doi: https://doi.org/10.1002/mp.12805
13. Zindler JD, Bruynzeel AME, Eekers DBP, Hurkmans CW, Swinnen A, Lambin P. Whole brain radiotherapy versus stereotactic radiosurgery for 4–10 brain metastases: a phase III randomised multicentre trial. *BMC Cancer* 2017; **17**: 1–5. doi: https://doi.org/10.1186/s12885-017-3494-z
14. Allgaier B, Schüle E, Würfel J. Dose reconstruction in the OCTAVIUS 4D phantom and in the patient without using dose information from the TPS. *PTW White Pap* 2013; **D913.200.0**: 0–7.
15. Depuydt T, Van Esch A, Huyskens DP. A quantitative evaluation of IMRT dose distributions: refinement and clinical assessment of the gamma evaluation. *Radiother Oncol* 2002; **62**: 309–19. doi: https://doi.org/10.1016/S0167-8140(01)00497-2
16. Poppe B, Stelljes TS, Looe HK, Chofor N, Harder D, Willborn K. Performance parameters of a liquid filled ionization chamber array. *Med Phys* 2013; **40**: 1–14. doi: https://doi.org/10.1118/1.4816298
17. Khan FM, Gibbons JP. *Khan's the physics of radiation therapy*. Philadelphia: Wolters Kluwer Health; 2014.
18. Wolfs CJA, Swinnen ACC, Nijsten SMJJG, Verhaegen F. Should dose from small fields be limited for dose verification procedures?: uncertainty versus small field dose in VMAT treatments. *Phys. Med. Biol.* 2018; **63**: 20NT01. doi: https://doi.org/10.1088/1361-6560/aae338
19. Swinnen ACC, Öllers MC, Roijen E, Nijsten SM, Verhaegen F. Influence of the jaw tracking technique on the dose calculation accuracy of small field VMAT plans. *J Appl Clin Med Phys* 2017; **18**: 186–95. doi: https://doi.org/10.1002/acm2.12029
20. Knill C, Snyder M, Rakowski JT, Zhuang L, Matuszak M, Burmeister J. Investigating ion recombination effects in a liquid-filled ionization chamber array used for IMRT QA measurements. *Med Phys* 2016; **43**: 2476–84. doi: https://doi.org/10.1118/1.4946822
21. Ohtakara K, Hayashi S, Tanaka H, Hoshi H. Consideration of optimal isodose surface selection for target coverage in micro-multileaf collimator-based stereotactic radiotherapy for large cystic brain metastases: comparison of 90%, 80% and 70% isodose surface-based planning. *Br J Radiol* 2012; **85**: e640–6. doi: https://doi.org/10.1259/bjr/21015703
22. Clark GM, Popple RA, Prendergast BM, Spencer SA, Thomas EM, Stewart JG, et al. Plan quality and treatment planning technique for single isocenter cranial radiosurgery with volumetric modulated Arc therapy. *Pract Radiat Oncol* 2012; **2**: 306–13. doi: https://doi.org/10.1016/j.prro.2011.12.003
23. Ohira S, Ueda Y, Akino Y, Hashimoto M, Masaoka A, Hirata T, et al. HyperArc VMAT planning for single and multiple brain metastases stereotactic radiosurgery: a new treatment planning approach. *Radiat Oncol* 2018; **13**: 1–9. doi: https://doi.org/10.1186/s13014-017-0948-z
24. Knöös T, Wieslander E, Cozzi L, Brink C, Fogliata A, Albers D, et al. Comparison of dose calculation algorithms for treatment planning in external photon beam therapy for clinical situations. *Phys Med Biol* 2006; **51**: 5785–807. doi: https://doi.org/10.1088/0031-9155/51/22/005
25. Fogliata A, Nicolini G, Clivio A, Vanetti E, Mancosu P, Cozzi L. Dosimetric validation of the Acuros xB advanced dose calculation algorithm: fundamental characterization in water. *Phys Med Biol* 2011; **56**: 2885–6. doi: https://doi.org/10.1088/0031-9155/56/9/2885
26. Makris DN, Pappas EP, Zoros E, Papanikolaou N, Saenz DL, Kalaitzakis G, et al. Characterization of a novel 3D printed patient specific phantom for quality assurance in cranial stereotactic radiosurgery applications. *Phys Med Biol* 2019; **64**: 105009. doi: https://doi.org/10.1088/1361-6560/ab1758